A 2.5 THz Receiver Front-End for Spaceborne Applications

M.C. Gaidis[a], H.M. Pickett, P.H. Siegel, C.D. Smith[b], R.P. Smith, S.C. Martin
Jet Propulsion Laboratory, California Institute of Technology, Pasadena, CA 91109

Abstract— **The OH radical is an important player in known ozone depletion cycles; however, due to its location in the atmosphere, it must be studied from either a balloon or spaceborne platform. For long-term mapping over large portions of the earth, a spaceborne platform is the most desirable. NASA's Earth Observing System Microwave Limb Sounder instrument is slated to house a 2.5 THz Schottky-diode receiver for such measurements. Here we describe the design, fabrication, and testing of the receiver front end. Selected components will be used in the first terahertz heterodyne receiver to be flown in space.**

I. Introduction

The OH radical plays a significant role in a great many of the known ozone destruction cycles, and has become the focus of an important radiometer development effort for NASA's Earth Observing System (EOS) Chem I satellite, which will monitor and study many tropospheric and stratospheric gases and is scheduled for launch in 2002 [1]. The Microwave Limb Sounder (MLS) instrument on this satellite is the only near-term opportunity to obtain global measurements of this important radical.

The lowest order OH doublets at 2510 and 2514 GHz fall fortuitously close to a strong methanol laser line at 2522 GHz. A receiver noise of 20,000 K, SSB is expected to provide enough sensitivity for daily global stratospheric maps of OH above 35 km and monthly global maps to 18 km from a limb-sounding satellite in polar orbit. These requirements are consistent with the performance that can be obtained from state-of-the-art room-temperature Schottky diode mixers. The molecular oxygen line at 2502 GHz can also be monitored as a pressure/altitude indicator.

The challenges of producing such sensitive mixers are numerous, but for this application, there is the added challenge of designing a robust receiver which can withstand the environmental extremes of a rocket launch and five years in low earth orbit. In this presentation, we discuss the design and implementation of the first terahertz heterodyne receiver scheduled to be flown in space.

II. Receiver Front End Design

The receiver front-end used to detect the OH radical at 2.5 THz consists of the following components and is schematically outlined in Fig. 1:

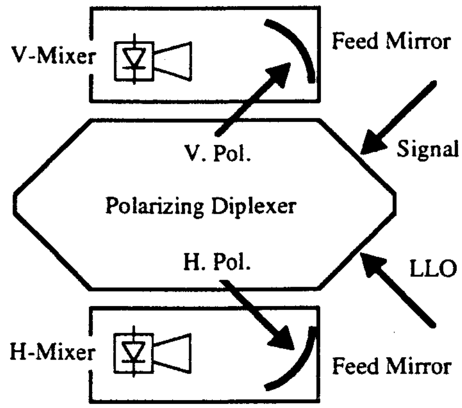

Fig. 1. Schematic diagram of the quasi-optical components in the 2.5 THz receiver front end.

- A diplexer to combine the OH signal and the laser local oscillator (LLO)
- Elliptical feed mirrors to shape the beams of the mixer feedhorns
- Fundamental Schottky-diode mixers for horizontal and vertical polarizations
- Support structures allowing simple, rugged alignment
- Low noise IF amplification chain (not pictured) from 7 to 22 GHz.
- Mixer bias circuitry (not pictured).

Note that the space-qualified LLO is a complex subsystem in itself, and is not included here as part of the front-end. However, it should be mentioned that the LLO technology is quite well developed, and will deliver more than 20 mW of 2.5 THz power for only 125 W of spacecraft power. The LLO is 75 x 30 x 10 cm in size, and 20 kg in mass [2].

A. Diplexer

The principle of operation of the protoflight model (PFM) diplexer is shown in Fig. 2. It is a dual-polarization four-port version of the commonly used Martin-Puplett diplexer. The diplexer's dual-polarization operation serves to lower the system noise by √2 and provide the redundancy important to space flight missions. (The atmospheric radiance is not expected to be significantly polarized.) The four-port configuration is made possible with an input grid (the right most grid in Fig. 2) which splits incoming radiation into two equal portions. The difference in path length between the two roof mirrors determines output polarization at a given intermediate frequency (IF). If just one signal IF were employed, it would be straightforward to optimize coupling of LLO and signal simultaneously. Unfortunately, for reasonable path length differences, one cannot simultaneously optimize coupling of the LLO and the three IFs of interest.

This is apparent from Fig. 3, which plots the sin-squared

---

[a] E-mail: gaidis@merlin.jpl.nasa.gov
[b] C.D. Smith is with Swales Aerospace, Pasadena, CA 91107.

We would like to acknowledge the many valuable contributions of the following people: J. Apodaca, P. Bruneau, T. Cox, T. Crawford, A. Deslis, V. Ford, D. Harding, T. Lee, C. Mann, E. Mueller, J. Oswald, A. Pease, J. Podosek, P. Stimson, R. Tsang, J. Voeltz, and U. Zimmerman.

This research was performed at the California Institute of Technology, Jet Propulsion Laboratory, under contract with the National Aeronautics and Space Administration's Office of Advanced Concepts and Technology and the Earth Observing System Microwave Limb Sounder Project Office.

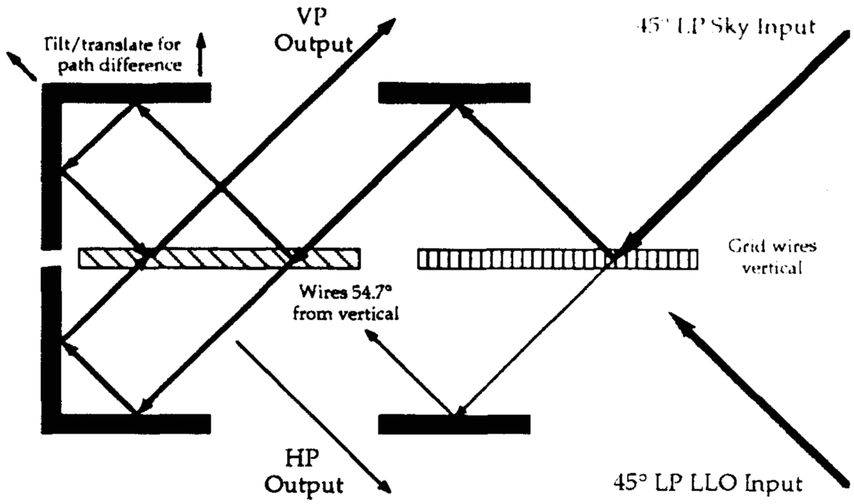

Fig. 2. Diplexer principle of operation. The right most grid splits the two input beams into two components for each beam. The heavy line follows the reflected half of the sky input (vertically polarized sky radiation). The left most grid splits this into two components, and interferometrically combines them after these two components are subjected to slightly different path lengths. The path length difference is adjusted such that the vertically polarized sky input at 12.8 GHz IF will pass through the "VP Output" port. Sky inputs at 8.4 and 20.4 GHz IF will exhibit some cross-pol component due to compromises in the choice of path length. The LLO appears nearly horizontal at the HP port and nearly vertical at the VP port.

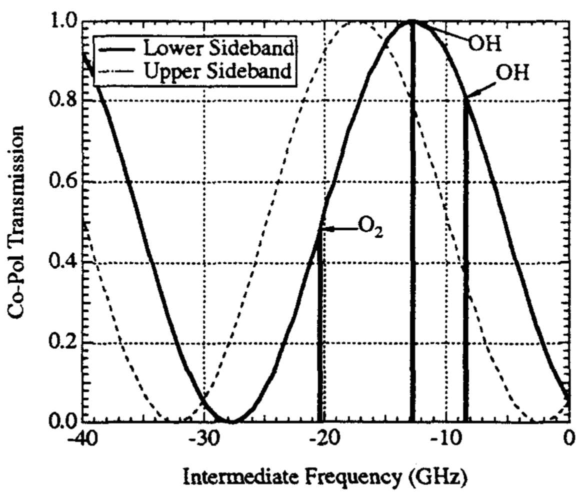

Fig. 3. Designed co-pol transmission of the sky signal through the 2.5 THz diplexer. The LLO beam will behave similarly, but with transmission curves identical to one minus the sky transmission. Note the opposite sideband rejection obtained for the OH channels by choice of path length difference (9.972 mm).

behavior of the diplexer with IF for our chosen nominal path length of 9.972 mm. Sensitivity is most important for the two OH IFs, but one cannot place the transmission peak directly between them without wiping out the oxygen signal. The nominal path length results ideally in 94% LO coupling, 82% coupling at 8.4 GHz IF, 99% at 12.8 GHz IF, and 49% at the less-critical 20.4 GHz oxygen line IF band. At 8.4 GHz IF, 82% of the HP mixer's beam will couple to horizontally polarized sky radiation, but the remaining 18% will come from vertically polarized radiation originating in the approximately constant 300 K LLO port. Although a folded Fabry-Perot type diplexer could be constructed to offer better coupling at all frequencies of interest simultaneously, stability and ease of use made the Martin-Puplett our first choice.

In practice, we fold the diplexer diagram of Fig. 2 into three dimensions so as to make a more compact, rugged design. The photograph in Fig. 4 shows the "VP" half of the diplexer, to which is mounted the two polarizing wire grids

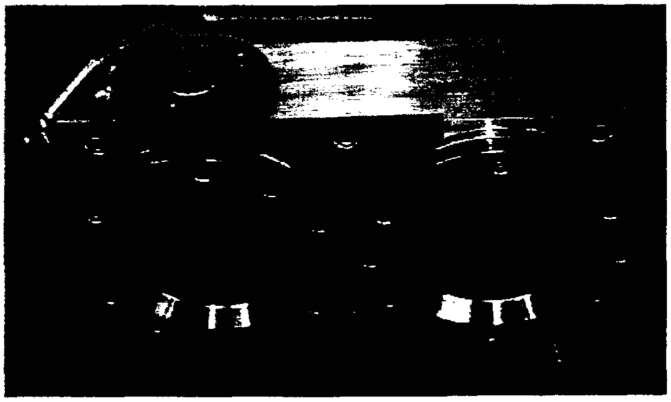

Fig. 4. Polarizing grids mounted on half of the 2.5 THz diplexer . The adjustable path length mechanism is visible in the upper left. The wheel presses against an invar spacer.

and the "adjustable" roof mirror. The two 45 mm free-aperture wire grid polarizers incorporate 5 μm diameter gold-coated tungsten wire on 12.5 μm centers in stainless steel frames [3]. The adjustable roof mirror is spaced from the diplexer body by the nominal distance of (9.972/2) mm with invar spacers. To allow for machining tolerances, a mechanism is used to give ± 200 μm in fine adjustment of this path length. The adjustment is accomplished with a circular "adjuster wheel" which rotates about a shoulder bolt 200 μm off-center. The wheel contacts one of the invar spacers, and is eccentrically rotated to tilt the rooftop mirror mount, causing a change in path length with a negligible effect on beam location. The wheel is made of aluminum with a Teflon-impregnated anodized coating, designed to withstand abrasion while rotating against the invar spacer. This mechanism is secured with epoxy before flight, and the rooftop mirror mount is spring-loaded against the wheel to withstand vibration.

Fig. 6 offers two views of the fully assembled PFM diplexer. The "HP" half of the diplexer is symmetrically spaced from the VP half with respect to the grids with stainless steel standoffs. The "fixed" roof mirror bolts directly to the HP half of the diplexer. The optical design

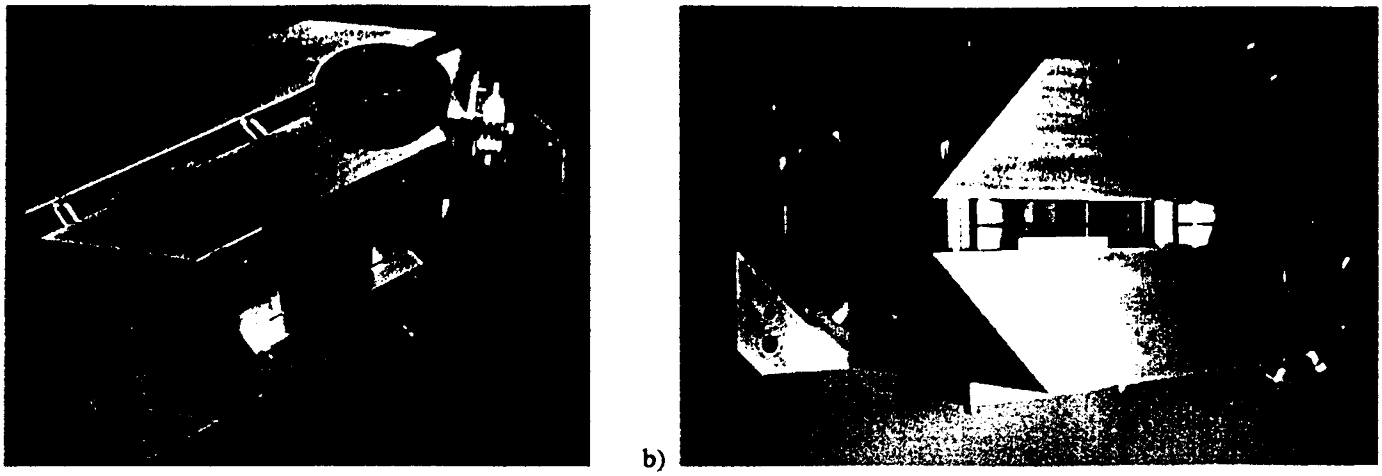

Fig. 6. Two views of the assembled 2.5 THz diplexer. In (a), one can see the LO input port at bottom left, the vertical-polarization output in the center, and the adjuster wheel with tilting roof mirror at the top right. Figure (b) shows the sky input at top left, a hint of the fixed roof mirror at top right, and the wire grid polarizer frames along the center.

places the beam waist (≈ 4.1 mm radius) close to the flat turning mirror visible at bottom center of Fig. 6a. Apertures of ≥ 22.5 mm diameter are used to avoid truncation effects. All components not previously discussed are made from the same alloy of aluminum to minimize effects due to thermal expansion. The design has been optimized for ruggedness, mass, volume, thermal stability, and alignment procedures.

B. Receiver Front End

The receiver front end components are pictured for the HP mixer in Fig. 7. The VP mixer is essentially identical, but with the mixer and IF chain flipped 90° clockwise, and the whole assembly mirror-imaged. The feed mirrors are diamond-turned off-axis ellipsoids which convert the rapidly diverging feedhorn beam to a well-collimated beam suited for best diplexer performance. The angle of incidence is 22.5°, a compromise between optimal on-axis operation and beam truncation requirements. The feed mirrors (and diplexer mirrors) are optically accurate, allowing the difficult receiver alignment to include the use of a HeNe

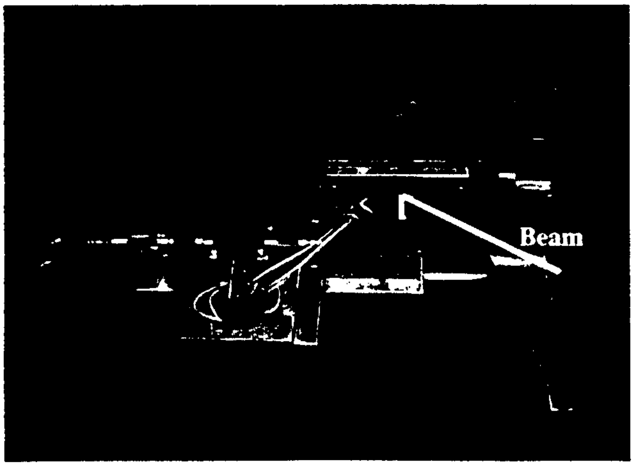

Fig. 7. Close-up of receiver front end components. The chain includes an off-axis elliptical feed mirror, the mixer, a 7 to 22 GHz IF amplifier, and a clamped attenuator. Thermometry, amplifier power, and DC bias for the mixer passes through the connector at bottom. The feed mirror support (FMS) face to the right bolts to a long edge of the hexagonal diplexer.

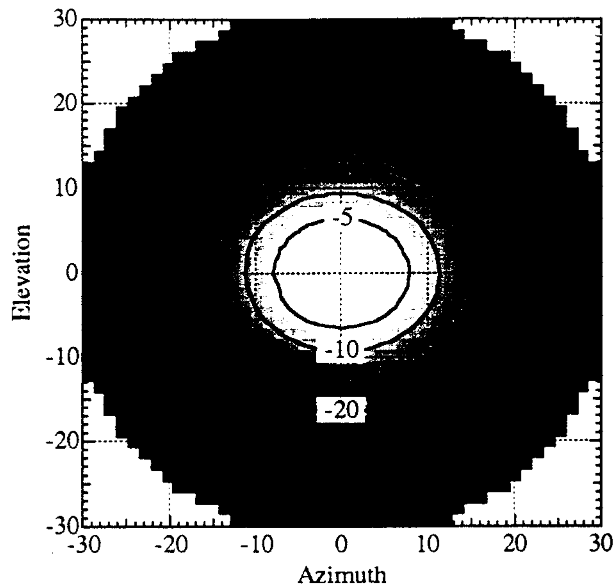

Fig. 5. JPL 2.5 THz Pickett-Potter horn beam pattern. Contours are in dB.

laser and an optical autocollimating alignment telescope.

We use dual-mode Pickett-Potter conical feedhorns [4] electroformed on aluminum mandrels. Fig. 5 and Fig. 8 show an image/contour plot and E- and H- plane cuts for one of the horns. To date, two JPL horns have been tested and found to be essentially identical in beam pattern. A nominally identical horn, fashioned from a stainless steel mandrel by the Rutherford Appleton Laboratory (RAL) gives slightly more symmetric beam patterns [5]. The cause of the asymmetry evident in these horns is not presently understood, but similar behavior has been seen for such horns if oversized for the test frequency [4]. Perhaps non-ideal electrical conductivity at the surface of the horn gives an apparent increase in the horn's "electrical" size.

The radiation collected by the feedhorn passes through a single-mode 2.5 THz rectangular waveguide which in turn feeds a mixer. The mixers are GaAs Schottky monolithic membrane diodes (MOMEDs), designed and fabricated at the Jet Propulsion Laboratory [6]. The mixers utilize a new

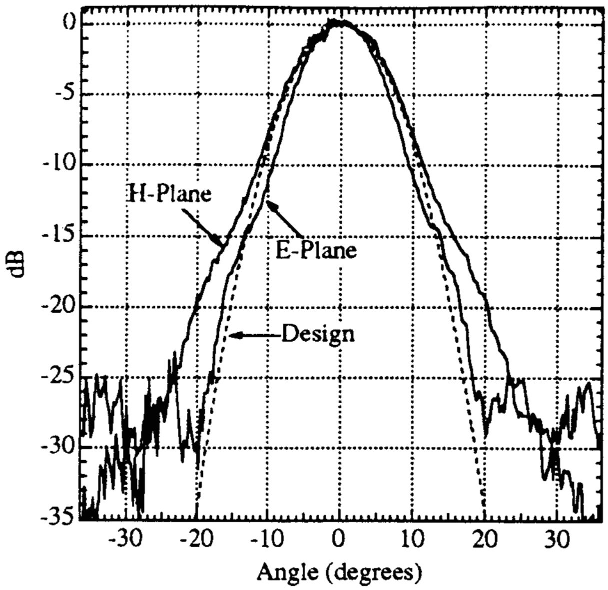

Fig. 8. JPL 2.5 THz Pickett-Potter horn beam pattern cuts in E– and H–planes, compared with the nominal design.

fabrication technique which offers more robust construction than existing whisker-contact corner-cube designs, while maintaining state-of-the-art noise performance. Comparable performance has been achieved as well with planar-whisker contacted waveguide mixers from RAL [7]. The LO power requirements of these mixers (≈ 5 mW) is modest enough to permit use of a low-power LLO. Fluctuations of laser power will be minimized through the use of three feedback loops, one of which uses the mixer DC signal to eliminate standing wave variations created by thermal changes as the spacecraft orbits the earth.

A resistive bias-tee arrangement has been chosen to protect the mixers while providing a DC bias path for the Schottky diode with minimal impact on the IF throughput. We have designed and implemented a differential feedback circuit to provide a stiff current bias with good immunity to noise pickup. The current bias also serves to reduce sensitivity of the device to LLO power fluctuations. A simple explanation is that, for an ideal Schottky diode, current bias is equivalent to curvature bias, and curvature is the dominant contributor to mixing as seen in a simple Taylor expansion argument. As shown in Fig. 9, for one of the JPL mixer designs, a factor of 4 change in LO power results in virtually no change of input noise temperature. Conversion gain behaves similarly. Other devices we have tested exhibit somewhat more sensitivity to LO power. Our thinking at present is that the IF transformer match is not as good for these other devices, and the LO power fluctuations result in device impedance changes which have non-negligible effect on the receiver characteristics. The IF transformer is a 7 - 22 GHz quartz suspended-substrate stripline step transformer, typically 100 Ω at the mixer end, and 50 Ω at the amplifier. Higher impedance transformers have been tested, offering better mode-matching to the MOMED output, but results have not been encouraging. We are now experimenting with alternative transformer materials and designs to offer good mode-matching and impedance matching simultaneously.

Low-noise (150 K at 8.4, 12.8 GHz, and 200 K at 20.4 GHz) IF amplifiers with AC-coupled inputs [8] amplify the downconverted mixer output by 32 dB. A 125 µm thick piece of indium is sandwiched between the amplifier and the mounting plate, and provides adequate heat-sinking for an operational temperature close to 30° C. The final component in the front end signal chain is a low-VSWR, broadband attenuator [9]. The attenuation value (typically 2 to 4 dB) is selected at test to provide the precise signal level required for best spectrometer sensitivity without saturation. A thermistor is located adjacent to the amplifier for diagnostic purposes.

III. 2.5 THz Mixer Test System

Accurate RF noise measurements at 2.5 THz are complicated by several factors: high mixer noise temperatures, variable atmospheric attenuation, poorly calibrated "absolute power" detectors, unavailability of matched attenuators, "gray" body loads, and imperfect Gaussian beams. The measurement test system used here to overcome these difficulties is schematically shown in Fig. 10. At this time, relatively few measurements have been made in demonstrating the successful operation of the flight-type diplexer, as a more flexible Martin-Puplett type diplexer [10] was used for earlier receiver measurements.

The noise temperatures are measured using the standard Y-factor technique on the full receiver only (that is, including the diplexer and atmospheric losses, and the addition of noise by the bias tee and the IF amplifier). A chopper switches the signal beam between a hot and a cold load during the measurement. A lock-in detector at the ≈

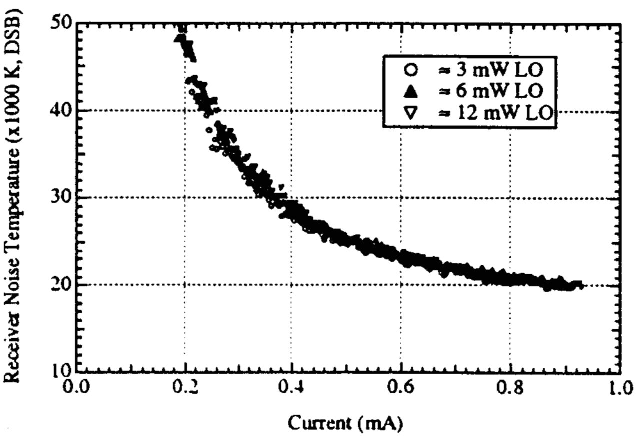

Fig. 9. Receiver noise vs. current at an IF of 8.4 GHz, demonstrating the use of current bias to reduce sensitivity to LO fluctuations. A factor of ≈ 4 in LO power results in virtually no input noise temperature change.

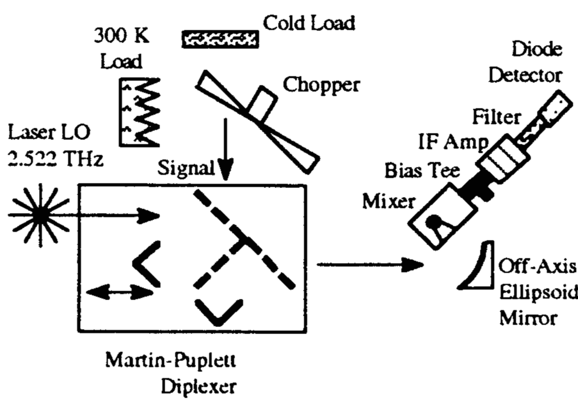

Fig. 10. Schematic of the 2.5 THz mixer test system. It is designed for sensitive measurement of high-noise devices, flexibility, and rapid computer-controlled measurements.

100 Hz chopper frequency extracts a hot/cold load power output variation from a crystal diode detector. A filter is placed in front of the crystal diode detector to select the IF band of interest: 8.4 GHz, 12.8 GHz, or 20.4 GHz. The filter bandwidth is ≈ 700 MHz.

After converting the lock-in signals from RMS to peak-to-peak values, we combine with the average DC output power to give the hot and cold powers needed for an accurate Y-factor calculation. This technique can be used to evaluate receivers with noise in excess of 500,000 K, DSB. It has been demonstrated that the noise temperature measured with the test system is consistent with that measured on the actual PFM diplexer.

IV. MOMED Schottky Diode Mixers

The Schottky-diode mixers and the mixerblock housings have been previously described [6]. To date, we have extensively RF tested 30 different devices of varying designs. The best devices are consistently of the same design, and devices of the same design offer very similar performance. Measured anode sizes of ≈ 0.35 μm x 1.0 μm on 10^{18} cm^{-3} material, and wide, tapered waveguide probes are the defining characteristics of the best MOMEDs. Smaller and larger anodes, and more narrow waveguide probes have been tested and give poorer performance. Our fabrication effort is now focussed on device yield and reliability for flight applications, although we are still experimenting with minor adjustments to the device design.

Fig. 11 compares receiver performance at 8.4, 12.8, and 20.4 GHz. The receiver performance measured here is competitive with that of the best reported in the literature [11], particularly when one considers the fine quality of the beam from the Pickett-Potter horn. The performance at 20.4 GHz is notably worse than at the other IF frequencies, in part because of amplifier noise. Although sideband ratio measurements have not yet been performed, the large RF/IF ratio would suggest that this should not account for the remainder of the differences between the three IF bands.

We presently believe the IF match to be the cause of performance variation between the IF bands. RF match may not be optimal either, but the similarity in appearance of the

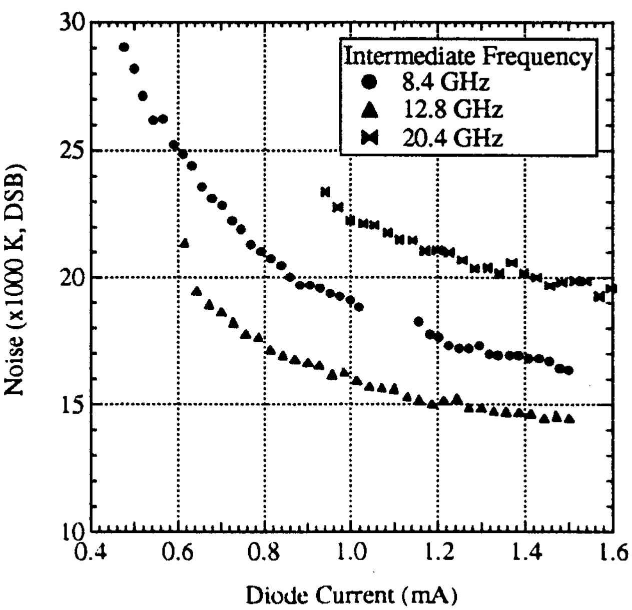

Fig. 11. Receiver noise vs. current at intermediate frequencies of 8.4 GHz, 12.8, and 20.4 GHz. Filters with bandwidth of ≈ 700 MHz were used to separate the intermediate frequencies. The LO power coupled to the mixer was approximately 8 mW.

three curves would suggest a relatively constant RF match across the full IF range. The slopes of the curves suggest that the combined RF and IF match is best at high current (low dynamic resistance). For this device, we also find the noise performance to degrade as LO power is reduced (reduction of LO power by a factor of ≈ 2 results in ≈ 5% to 10% noise increase). Better performance at higher LO power also suggests the need to lower the mixer impedance. However, we find lower noise temperatures when using lower impedance IF transformers. It seems that the waveguide probe configuration wants a lower impedance device for best RF match (or wider probe for constant impedance), but the IF transformer is presently tuned to match a higher impedance device. We have not been able to test transformers with less than 100 Ω input impedance, and are somewhat wary of mode matching between the very small MOMED beam lead and the huge 100 Ω quartz section. Indeed, network analyzer measurements of the return loss looking in the mixer output port show significant variation across the full IF range, and show dramatic sensitivity to the quality of the wirebond connections made within the mixer block. We have started the fabrication and testing of new IF coupling structures which should alleviate these problems.

V. Qualification for Spaceflight

Although it is possible to create a low noise terahertz receiver in the laboratory, a serious challenge exists in making it robust enough for practical use. Much effort has gone into the design of the receiver front end so that it will withstand the environmental extremes of vibration during launch. It is yet another chore to ensure the 5 year lifetime of the mission. The nature of the device and its mounting fixtures make the other environmental effects less difficult to deal with: thermal, vacuum, and radiation effects are not a serious problem in the EOS-MLS spacecraft.

The spaceflight qualification of the front end began with a balloon flight of a breadboard model front end. The front end performed without a problem, and some useful OH measurements were performed [12]. A gondola coolant pump failure prevented extensive data collection.

To further establish the reliability of the mixers, the mixer blocks were subjected to thermal testing. Rapid thermal cycling (4 cycles from -50 C to +100 C, 20 min dwell times at each extreme) was performed on 6 devices, and found to have no noticeable effect on the DC device characteristics. As thermally-induced damage is potentially the most difficult problem to circumvent, the test results offer a good deal of reassurance that the JPL MOMED mixers will perform well in a flight environment. The predicted flight survival temperature range for the EOS-MLS THz receiver front end is from -30° C to +55° C.

The small size of the MOMED mixers makes them relatively insensitive to the low-frequency vibration experienced during launch. The rest of the front end is quite susceptible to damage. To test the robustness of the design, the assembled front end was subjected to the following random vibration, for 3 minutes each in x, y, and z axes (expected to mimic the launch environment):

20 - 50 Hz	+6 dB/octave
50 - 500 Hz	0.2 g^2/Hz
500 - 2000 Hz	–6 dB/octave
Overall	13.0 g (rms).

Fig. 12 shows the assembled front end on the z-axis shake table. The front end survived vibrational testing quite well, with the only defect noted to be the cracking of a

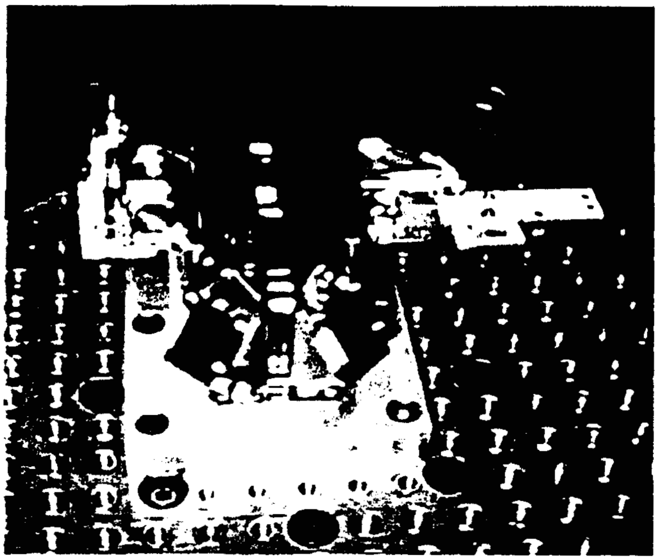

Fig. 12. Assembled receiver front end, mounted on the electrodynamic shake table. Note the "vertical" mixer on the left, and the "horizontal" mixer on the right. The diplexer adjuster wheel is atop the roof mirror on the left.

substandard epoxy joint used to secure the horizontal mixer block SMA connector. RF coupling, noise temperature, and DC I-V characteristics were otherwise identical before and after the test.

The burden of operation in a vacuum environment primarily places requirements on the types of epoxies allowed, and on the thermal difficulties due to lack of convection. Simulations have been performed to estimate temperatures around the receiver front end, and predict no problems. The diplexer is designed to be insensitive to temperature, and harmful thermal gradients are minimized.

The predicted total radiation dose over the 5 year mission life is 60 krad (Si). Proton irradiation of the device will not be an issue because it is surrounded by ≈ 5 mm of brass mixerblock. In addition, GaAs diodes are known to be relatively immune to total-dose effects resulting from the deposition of ionizing energy [13].

To ensure mixer lifetimes in excess of the 5 year mission, accelerated lifetests with fit to an Arrhenius-lognormal degradation are planned to begin in mid 1999. Parameters used to define a device failure are expected to include I_{sat}, R_s, η, as well as the low-frequency noise signature of the device. It is hoped that one can use the low frequency noise as a diagnostic as well as a measure of degradation [14].

VI. Summary

Excellent performance of fixed-tuned Schottky-diode receivers in a robust, stand-alone receiver configuration has been demonstrated. Receiver noise of better than 14,500 K, DSB has been measured for JPL MOMED mixers at 12.8 GHz IF and 2.5 THz RF. High-quality beam patterns in close agreement with theory have been measured at 2.5 THz on Pickett-Potter dual-mode horns. This noise and beam quality is required for monitoring of atmospheric chemistry, and can facilitate the development of several important remote-sensing and in-situ applications [15]. With the concurrent development of low-power, compact THz laser local oscillators, this technology is realizable in a spaceborne platform. Work in the near future will concentrate on integration of the EM and PFM components, noise temperature reduction, environmental testing, and device lifetime testing.

VII. References

[1] J.W. Waters, "The Chlorine Threat to Stratospheric Ozone," *Engineering and Science*, 3 - 13 (Summer, 1993); Pickett HM, Peterson DB, "Comparison of Measured Stratospheric OH with Prediction," *J. Geophys. Res.-Atm.*, **101**, 16789-16796 (1996); J.M. Russell, *et al.*, "The Halogen Occultation Experiment," *J. Geophys. Res.-Atm.*, **98**, 10777-10797 (1993).

[2] E.R. Mueller, W.E. Robotham, Jr., R.P. Meisner, R.A. Hart, J. Kennedy, and L.A. Newman, "2.5 THz Laser Local Oscillator for the EOS Chem 1 Satellite," *Proc. 9th Int'l Symp. on Space THz Tech.*, Pasadena, CA, 563 - 572 (1998).

[3] Graseby Specac, 500 Technology Court, Smyrna, GA 3008

[4] H.M. Pickett, J.C. Hardy, and J. Farhoomand, "Characterization of a Dual-Mode Horn for Submillimeter Wavelengths," *IEEE Trans. Micr. Theory Tech.*, **32**, 936 - 937 (1984).

[5] D.S. Wilsher, J.J. Spencer, C.M. Mann, M.C. Gaidis, "A Moderate Cost 2.5 THz High Performance Feedhorn," to be presented at the *10th Intl. Symposium on Space THz Tech.*, Charlottesville, VA, March 16-18, 1999.

[6] P.H. Siegel, R.P. Smith, M.C. Gaidis, and S. Martin, "2.5 THz GaAs Monolithic Membrane-Diode Mixer," to be published in *IEEE Trans. Micr. Theory Tech.*, 1999.

[7] B.N. Ellison, B.J. Maddison, C.M. Mann, D.N. Matheson, M.L. Oldfield, S. Marazita, T.W. Crowe, P. Maaskant, and W.M. Kelly, "First Results for a 2.5 THz Schottky Diode Waveguide Mixer," *Proc. of the 7th Intl. Symposium on Space THz Tech.*, Charlottesville, VA, 494 - 502 (1996).

[8] Miteq model JSD2-00010, Miteq Inc., 100 Davids Drive, Hauppauge, NY 11788

[9] Weinschel model 56, Weinschel Corp., 5305 Spectrum Drive, Frederick, MD 21703-7362

[10] Thomas Keating, Ltd., Station Mills, Billingshurst, West Sussex, RH14 9SH, England

[11] H.P. Roser, H.W. Hubers, T.W. Crowe, and W.C.B Peatman, "Nanostructure GaAs Schottky Diodes for Far-Infrared Heterodyne Receivers," *Infrared Phys. Technol.*, **35**, 451 - 462 (1994).

[12] H.M. Pickett, "THz Spectroscopy of the Atmosphere," presented at *SPIE's Intl. Symposium on High Power Lasers and Applications*, San Jose, CA, January 23-29, 1999.

[13] S. Kayali, G. Ponchak, and R. Shaw, "GaAs MMIC Reliability Assurance Guidelines for Space Applications," JPL Publication 96-25 (1996).

[14] L.K.J. Vandamme, "Noise as a Diagnostic Tool for Quality and Reliability of Electronic Devices," *IEEE Trans. Electron. Devices*, **41**, 2176 - 2187 (1994).

[15] E.R. Mueller, personal communication.